HHS Public Access

Author manuscript

Eur J Med Genet. Author manuscript; available in PMC 2023 June 01.

Published in final edited form as:

Eur J Med Genet. 2022 June ; 65(6): 104497. doi:10.1016/j.ejmg.2022.104497.

Novel biallelic variants affecting the OTU domain of the gene OTUD6B associate with severe intellectual disability syndrome and molecular dynamics simulations

Sultan Cingoz[a,b,*], **Didem Soydemir**[c,1], **Tülay Oncü Oner**[a,1], **Ezgi Karaca**[d,e], **Burcu Ozden**[d,e], **Semra Hız Kurul**[c,d], **Erhan Bayram**[c], **University of Washington Center for Mendelian Genomics**[b], **Bradley P. Coe**[b], **Deborah A. Nickerson**[b], **Evan E. Eichler**[b,f]

[a]Department of Medical Biology and Genetics, Faculty of Medicine, Dokuz Eylul University, Izmir, Turkey

[b]Department of Genome Sciences, University of Washington School of Medicine, Seattle, WA, USA

[c]Department of Pediatrics, Division of Child Neurology, Faculty of Medicine, Dokuz Eylul University, Izmir, Turkey

[d]Izmir Biomedicine and Genome Center, Dokuz Eylul Health Campus, Izmir, Turkey

[e]Izmir International Biomedicine and Genome Institute, Dokuz Eylul University, Izmir, Turkey

[f]Howard Hughes Medical Institute, University of Washington, Seattle, WA, USA

Abstract

Intellectual developmental disorder with dysmorphic facies, seizures, and distal limb anomalies (IDDFSDA) is an autosomal recessive multisystem disorder caused by compound heterozygous or homozygous variants in the gene *OTUD6B*. Herein, we describe novel pathogenic compound heterozygous variants in *OTUD6B* identified via whole-exome sequencing in an index case

[*]**Corresponding author.** Department of Medical Biology and Genetics, School of Medicine, Dokuz Eylul University, 35340, Inciralti, Izmir, Turkey. sultan.cingoz@deu.edu.tr (S. Cingoz).

[1]These authors contributed equally to this work.

Author's contribution

Conceptualization: S.C., E.E.E.; Data curation: S.C., B.P.C, UW-CMG; Formal Analysis: S.C., B.P.C; Funding acquisition: S.C., E.E.E., D.A.N.; Investigation: S.C.; Resources: S.H.K., D.S., E.B.; Methology: S.C., T.O.O., B.O.; Validation; T.O.O., B.O., E.K.; Project administration: S.C., E.E.E; Software: B.P.C, UW-CMG., E.K.; Visualization: D.S., T.O.O.; Supervision: S.C.; Writing – original draft: S.C.; Writing – review & editing: E.E.E., D.A.N.

Ethical approval and consent to participants

Written informed consent was obtained from the parents of the index case.

Consent for publication

Consent for publication was obtained from the parents of the index case.

Availability of data and material

All data generated or analyzed during this study is included in the final published article.

Declaration of competing interest

The authors declare that there are no competing interests.

exhibited the severe IDDFSDA phenotype. The potential pathogenicity of the novel frameshift and missense variants in the index case was investigated using *in silico* tools. The truncating frameshift variant in one allele was predicted to undergo degradation via nonsense-mediated decay of the mRNA molecule. To predict the severity of the damage to the protein caused by the missense variant in the other allele and its effects on phenotypic severity was further investigated together with a previously reported first homozygous missense variant in the same domain in another patient with a less severe IDDFSDA phenotype using structural modeling and molecular dynamics (MD) simulations for the first time. Based on these analyzes, it is anticipated that Tyr216Cys in the earlier reported case with less severe IDDFSDA will lead to localized destabilization, whereas Ile274Arg in the presented index case with the severe IDDFSDA phenotype will lead to significant distortion in the overall fold of OTUD6B. Our findings suggest that compound LOF and ultrarare missense variants may be contribute to the underlying variability expressivity associated with this disorder. In conclusion, our findings support that the clinical severity could be related with the predicted functional severity of the variations in OTUD6B. However, additional functional studies are required.

Keywords

OTUD6B ; OTU domain; severe IDDFSDA; molecular dynamics simulations; missense variant

1. Introduction

The gene *OTUD6B* (OTU deubiquitinase 6B) is located on chromosome 8q21.3 and includes seven exons (Online Mendelian Inheritance in Men, OMIM, #612021). *OTUD6B* encodes a member of the ovarian tumor domain (OTU) containing the subfamily of deubiquitinases (DUBs), which are proteases that specifically cleave ubiquitin linkages (Kayagaki et al., 2007; Komander and Barford, 2008; Komander et al., 2009; Xu et al., 2011; Mevissen et al., 2013). The OTU-type DUBs link the ubiquitin chains using conserved residues (ubiquitin-binding pockets) in their OTU domain. In all, 16 of the 18 OTU-type DUBs genes contain an intact catalytic triad (Xu et al., 2011; Mevissen et al., 2013). The catalytic triad—or core catalytic domain—is important not only for OTU-type DUBs containing the OTU domain, but also for all other cysteine protease genes.

Biallelic pathogenic variants described in *OTUD6B* in 20 individuals from 11 unrelated families have been associated with intellectual developmental disorder with dysmorphic facies, seizures, and distal limb anomalies (IDDFSDA) (Table 1) (Online Mendelian Inheritance in Men, OMIM, #617452). According to reports, it exhibits an autosomal recessive transmission pattern disorder (Santiago-Sim et al., 2017; Straniero et al., 2018; Alkuraya et al., 2020; Phetthong et al., 2021; Abdel-Salam et al., 2022). The disorder covers a wide clinical phenotypic spectrum of different severity. A limited number of recent studies show that the most severe form of IDDFSDA have severe intellectual disability syndrome, epilepsy, and multiple congenital anomalies consisting of dysmorphic facial appearance, structural brain abnormalities, including corpus callosum hypoplasia, white matter volume loss, and dilatation of the lateral ventricles (Santiago-Sim et al., 2017; Abdel-Salam et al., 2022). On the other hand, the patients with less severe clinical phenotype have mild to

moderate intellectual disability with normal speech and motor development (Santiago-Sim et al., 2017; Straniero et al., 2018; Abdel-Salam et al., 2022).

Herein, we report novel compound heterozygous variants associated with IDDFSDA; a frameshift (p.Val206fs) and a missense (p.Ile274Arg) in the deubiquitinating enzyme gene *OTUD6B* that were identified via whole-exome sequencing in the index case and non-consanguineous parents, and confirmed via Sanger sequencing. The truncating frameshift variant (NP_057107.4:p.Val206fs) in one allele was predicted to undergo degradation via nonsense-mediated decay of the mRNA molecule. To predict the severity of the damage to the protein caused by the missense variants in *OTUD6B*, structural modeling and molecular dynamics simulations were performed for the first time. The effect of amino acid substitutions both previously published (p.Tyr216Cys) and in the present study (p.Ile274Arg), on the structure of the OTUD6B protein were evaluated together to compare the effect of the missense variants on OTUD6B protein structure and function, and to predict the relationship between genotype and phenotypic severity.

2. Materials (subjects) and methods

2.1. Editorial policies, ethical considerations, and DNA extraction

This study protocol was approved by the Dokuz Eylul University Ethics Committee and written informed consent was obtained from the parents of the index case. Genomic DNA was extracted from peripheral blood using a NucleoSpin® Blood L Kit (Macherey-Nagel, Duren, Germany), according to the manufacturer's instructions.

2.2. Clinical report

The index case (a 17-year-old male) presented to our pediatric neurology department at age 12 years due to developmental delay, intractable seizures, and multiple congenital anomalies, including congenital heart disease, renal malformation, and severe scoliosis. Anamnesis showed that he was the second child of nonconsanguineous parents. He was born at 32 weeks of gestation via emergency caesarian section due to fetal distress and intrauterine growth restriction (IUGR). He had a low APGAR score and was transferred to the neonatal intensive care unit (NICU) with respiratory insufficiency. He did not require assisted ventilation; however, additional investigations were performed following observation of dysmorphic features, including hypotelorism, midfacial hypoplasia, and a high-arched palate, and microcephaly.

Multisystemic diagnostic work up while hospitalized showed multiple congenital anomalies, encapsulating horseshoe kidneys, tetralogy of Fallot, and inguinal hernia. In terms of neurodevelopment milestones, he was able to sit up without support and walk at the age of 15 months and 3 years, respectively. Additionally, scoliosis was observed as a new neurologic sign when he was 3 years old.

The patient also had epilepsy based on his positive family history. The patient initially had generalized tonic clonic seizures at age 8 months. Phenobarbital 5 $mg \cdot kg^{-1} \cdot d^{-1}$ was initiated as the antiepileptic drug. EEG showed bilateral sharp waves were predominantly in the right centro-temporo-parietal regions, but seizure control with monotherapy was not successful.

Valproic acid 20 mg·kg^{-1}·d^{-1} was added to his treatment regimen and gradually increased to 40 mg·kg^{-1}·d^{-1}. For the clusters of seizure with similar semiology phenobarbital therapy was replaced by levetiracetam (from 15 mg·kg^{-1}·d^{-1} to 35 mg·kg^{-1}·d^{-1}). The seizures continued, though less frequently, and were stabilized by dual therapy until he was 8 years old. Laboratory tests, neuroradiological and neurophysiological studies were performed to determine the etiology of the patient's seizures and multiple congenital anomalies. Cranial MRI indicated right thalamic focal encephalomalacia and partial agenesis of the corpus callosum.

Recent EEG showed multiple epileptic abnormalities, including sharp slow wave discharges in the right frontotemporal and left parietooccipital regions that were observed 2-3 times during a 20-s period (marked by black arrows in Fig. 1A, B). At the time of the patient's most recent evaluation at age 17 years his anthropometric measurements were as follows: weight: 29 kg (−6 SDS); height: 140 cm (−5.15 SDS); head circumference 51 cm (−4.4 SDS). In addition, he could not sit unsupported or walk independently. Although he knew a few words when he was 7 years old, he was getting worse and had no speech in the end. In addition, neurological examination showed notable axial hypotonia, with decreased muscle strength. He had prominent spasticity and increased deep tendon reflexes in the upper and lower extremities. He also had dysmorphic features (detailed in Table 1) with skeletal deformities (Fig. 2A, B). At the time this manuscript was prepared he was aged 17 years and had been seizure free with a dual antiepileptic treatment regimen (valproic acid and levetiracetam) for 6 months.

2.3. Genomic analysis

The standard genetic diagnosis approach in cases of intellectual disability (ID) was applied. After conventional cytogenetic analysis by G- banding in index case, genome-wide analysis of the copy number variants (CNVs) using array comparative genomic hybridization (aCGH) and a custom NimbleGen oligonucleotide array including 135,000 probes (53,068 for hotspots region and 81,932 for the genome) was initially performed. CNVs were called using a Hidden Markov model (HMM). CNVs were filtered according to American College of Medical Genetics (ACMG) criteria for molecular diagnosis (Matthijs et al., 2016).

2.4. Exome sequencing and analysis

Exome sequencing was performed in the index case and his parents, who had normal karyotype and array CGH results. The NimbleGen SeqCap EZ Human Exome Kit v2.0 was used for exome capture. Samples were sequenced with paired-end 50-bp reads using an Illumina HiSeq2000 sequencing platform and exome variants were called by the UWG-CMG GATK (Genome Analyzer Toolkit) pipeline (version date Dec 2015) and annotated via VEP v.83 (Variant Effect Predictor). Then, data were analyzed using GEMINI v.0.19.1 and suspected variants were screened in the following databases: dbSNP (https://www.ncbi.nlm.nih.gov/snp); ESP6500 (v2) (http://evs.gs.washington.edu/EVS/); 1000 Genomes (phase 3) (http://www.1000genomes.org/); ExAC (r0.3) (http://exac.broadinstitute.org/about); UK10K (Feb, 2016) (https://www.uk10k.org).

Variants with a frequency >0.005 in any single population within the ESP 6500 (v2), 1000 Genomes (phase 3), ExAC (r0.3) or UK10K (Feb, 2016) databases were excluded; this is referred to as maxAAF throughout this manuscript. Calls with genotype quality <20 (GQ < 20) and calls with read depth <6 (DP < 6) were excluded. After the variants in the family had been filtered, the disease candidate variants were selected using possible standard Mendelian models (homozygous recessive, compound heterozygous, X-linked recessive, X-linked de novo, and autosomal de novo). Rare variants (low minor allele frequency in the gnomAD variome) (http://gnomad.broadinstitute.org) were the focus of investigation. Potentially damaging variants were prioritized according to the American College of Medical Genetics Organization (Matthijs et al., 2016; Richards et al., 2015). *OTUD6B* (GenBank: NM_016023.3, GRCH37/hg19), including two heterozygous nonsynonymous variants, was prioritized as a likely pathogenic according to variant allele frequencies, genotype frequencies, inheritance models, family history, index case phenotype, gene functions, protein expression, and assessment using *in silico* prediction tools. After reviewing information available in the literature and databases, including OMIM, Monarch Initiative, and GeneCards, we identified what was considered to be the best candidate gene in the study family. There were no other candidate genes in this family.

As a result of the analyses, variants in *OTUD6B* were identified and further investigated. Variants in *OTUD6B* were not detected in control DNA samples. Variants and inheritance was validated via Sanger sequencing. The oligonucleotide primers used for PCR amplification and Sanger sequencing were as follows: OTUD6B-F, 5' AAT ATT GGC AGC TAG ACA G 3' and OTUD6B-R, 5' ATC TGG GTT CTT CTT ACG 3' for the frameshift variant, and OTUD6B-F, 5' GCC AAG ACT GCC GTG TTT 3' and OTUD6B-F, 5' CTC CCA GGG TGA CTG TCA TT 3' for the missense variant.

2.5. *In silico* prediction methods

2.5.1. *In silico* bioinformatics approaches using DNA sequence, protein sequence, and structural information—

First, we investigated the evolutionary conservation of the amino acid sequence of OTUD6B. We searched all homologs of OTUD6B sharing >35% sequence identity and then aligned them to disclose all possible amino acid changes in the sequence using the ConSurf server (Landau et al., 2005). A comparative analysis in 10 species of OTUD6B amino acid sequences was performed using ClustalW software (http://www.clustal.org/) (Fig. 3C).

The potential pathogenicity of the present (p.Ile274Arg) and a previously reported missense variants (p.Tyr216Cys) were assessed via 5 *in silico* approaches: Mutation Taster (http://www.mutationtaster.org/), SIFT (https://sift.bii.a-star.edu.sg/), PROVEAN (http://provean.jcvi.org/index.php), SNAP2 (http://www.rostlab.org/services/SNAP), and I-Mutant (http://folding.biofold.org/i-mutant/i-mutant2.0.html) (Supplementary Table 1).

The effect of the frameshift variant (p.Val206Glyfs*9) was evaluated via the Mutation Taster (http://www.mutationtaster.org/) and NMDEscPredictor (https://nmdprediction.shinyapps.io/nmdescpredictor/) databases.

2.5.2. Structural modeling and molecular dynamics (MD) simulations—The molecular dynamics simulations were performed with Gromacs 2020 (Abraham et al., 2015) under the effect of an AMBER99SB-ILDN force field. Water was modelled using TIP3P parameters and ionization was performed using NaCl at 0.15 M. The simulation box was set as a dodecahedron and the temperature was maintained at 310K during the 200-ns simulation.

3. Results

3.1. Exome sequencing and analysis

We identified novel compound heterozygous variants in the deubiquitinating enzyme gene *OTUD6B* via exome sequencing in the index case and non-consanguineous parents who had normal karyotype and array CGH results, and confirmed via Sanger sequencing.

According to the Mendelian models used, each parent for novel variants in *OTUD6B* were denoted as heterozygous (one alternate allele), and affected cases were denoted as compound heterozygous where the alleles are located at two different loci within the same gene (Fig. 3A). The index case carried two novel variants (NM_016023.3)—a paternally inherited frameshift variant [(NM_016023.3:c.617_618del) (NP_057107.4:p.Val206Glyfs*9)] (ClinVar accession number: SCV002061910) and a maternally inherited missense variant [(NM_016023.3:c.821 T>G) (NP_057107.4:p.Ile274Arg)] (ClinVar accession number: SCV002064127) located in exon 4 and exon 6 of *OTUD6B*, respectively (Figure 3A, B) (http://www.ncbi.nlm.nih.gov/clinvar). The missense variant c.821T>G was not reported in gnomAD. The frameshift variant c.617_618del is annotated in dbSNP 153 (rs1472577530) and the maximum subpopulation allele frequency (maxAAF) was 0.000008314 (2/240562 alleles, GnomAD_exome). A homozygous state was not detected in gnomAD. The CADD score was not available because it is an indel. The heterozygous private missense variant with a CADD score of 24.3 was private; this variant has not been previously reported in any population. Allele frequencies were obtained from the gnomAD database (https://gnomad.broadinstitute.org/) (Table 1).

3.2. *In silico* bioinformatics approaches using DNA sequence, protein sequence, and structural information

To understand the severity of the damage to the protein caused by the missense variant in the other allele and its effects on phenotypic severity using structural modeling and molecular dynamics (MD) simulations, the variant [NP_057107.4:p.Ile274Arg] was further investigated together with a previously reported first missense variant (p.Tyr216Cys) in the same domain in another patient with a less severe IDDFSDA phenotype.

In the evolutionary conservation analysis of the amino acid sequence of OTUD6B, it was noted that the Tyr216 position in the previously reported case can only be changed to the His, Ile, Phe, Arg, Ser, and Ile274 position, whereas in the presented case it can only be changed to Val and Lys evolutionarily. This implies that Tyr216Cys and Ile274Arg might not be evolutionary tolerated.

The potential pathogenicity of the present (p.Ile274Arg) and a previously reported missense variants (p.Tyr216Cys) were assessed via 5 *in silico* approaches. Mutation Taster, SIFT, PROVEAN, and SNAP2 suggested that the missense variant has a damaging/disease-causing effect on OTUD6B. The *in silico* prediction of the maternally inherited missense was that it was harmful [Mutation Taster "Disease causing" (probability: 0.9999); PROVEAN "Deleterious" (score: −5.360 [cutoff: −2.5]); SIFT "Damaging" (score: 0); SNAP2 "Effect" (score: 81; accuracy: 91%)] (Supplementary Table 1). Additionally, I-Mutant further indicated that this missense variant can decrease protein stability. On the other hand, the Mutation Taster database prediction for the frameshift variant was that it is disease-causing (probability: 1). According to the NMDEscPredictor database, p.Val206Glyfs*9 is predicted to undergo degradation via nonsense-mediated decay (NMD+). The novel variants in the index case with a severe IDDFSDA phenotype and previously reported missense variant in the same domain in another patient with a less severe IDDFSDA phenotype were predicted to be rare and pathogenic via 5 *in silico* approaches.

3.3. Thorough investigation of the effect of missense variants on the structure and function of the OTUD6B protein based on molecular dynamics and structural modeling

In the presented case the aim was to dissect the effect of Tyr216Cys and Ile274Arg substitutions on protein activity. In order to understand the effect of these variations, the 3D structure of OTUD6B was modeled (as its structure is not yet resolved). For modeling OTUD6B, we searched for structurally resolved OTUD6B homologs. The closest homolog shares ~10% sequence identity with OTUD6B (https://www.rcsb.org/structure/5LRW). Despite this low sequence similarity, we proceeded with the available template and obtained the wild type, Tyr216Cys variant, and Ile274Arg variant OTU domain models of OTUD6B by using the HHpred (Zimmermann et al., 2018) and Modeller (Webb and Sali, 2016) servers. The obtained structures and variation locations in the catalytic triad are depicted in Figure 4. Figure 4C shows that in the wild-type form, Tyr216, is surrounded by aromatic amino acids, leading to an aromatic packing, which is lost in the case of Tyr216Cys. Figure 4D represents that Ile274 is surrounded by hydrophobic amino acids that will be strongly destabilized upon Ile274Arg variation. So, expanding on the obtained models, it is expected that the variations cause stability problems in the protein, supported also by the protein stability prediction servers, MaestroWeb (Laimer et al., 2015) and DUET (Pires et al., 2014). According to the MaestroWeb Server, the stability changes for Tyr216Cys and Ile274Arg are predicted to be 0.792 kcal moL^{-1} and 2.564 kcal mol^{-1}, respectively. This indicates that both substitutions cause instability in the OTU domain, although Ile274Arg substitution leads to a more drastic change. DUET server results also validate this result, with more significant change in Ile274Arg substitution. These observations were also validated by running a more sophisticated simulation tool, i.e., molecular dynamics simulations. The Ile274Arg variant protein unfolded through simulation and a stable structure was never obtained, which implies that the change introduced by arginine is structurally incompatible with the hydrophobic core of the protein. As such, it was hypothesized that Tyr216Cys will lead to localized destabilization, whereas Ile274Arg will lead to significant distortion in the overall fold of OTUD6B.

4. Discussion

Exome sequencing is a powerful method for identifying genetic causes of neurodevelopmental disorders (Rump et al., 2015). Herein we reported novel compound heterozygous pathogenic variants in *OTUD6B* using trio-based exome sequencing in a patient with a severe neurodevelopmental disorder. Recently, biallelic variants in *OTUD6B* have been reported to cause IDDFSDA, characterized by a wide clinical spectrum (Santiago-Sim et al., 2017). To date, only 11 *OTUD6B* variants have been described in 20 cases from 11 families, with the exception of the variants described herein (Table 1 and Fig. 3B, C, D). Among the gene variants, 4 were discovered by Santiago-Sim et al. (2017); 1 homozygous nonsense variant (NM_016023.3:c.433 C>T) in exon 4 resulting in an Arg145-to-ter (p.Arg145*) substitution, 1 homozygous frameshift variant (NM_016023.3:c.469_473delTTAAC) (p.Leu157Argfs*8) in exon 4, 1 splice-site homozygous variant (NM_016023.3:c.173–2A>G) in intron 1 in which *OTUD6B* deletion leads to A to G transition in intron 1 of *OTUD6B* deletion, and 1 homozygous missense variant (NM_016023.3:c.647A>G) in exon 4 resulting in Tyr216 to Cys216 substitution (p.Tyr216Cys). Other homozygous nonsense variant (NM_016023.5:c.631G>T) (p.Glu211*), also referred to as (NM_016023.3:c.721G>T) (p.Glu241*), in exon 5 was discovered by Alkuraya et al. (2020). Straniero et al. (2018) described another patient with a milder phenotype and first compound heterozygous splice site variants (C.324+1G >C) and (C.405+1G >A) in *OTUD6B*. They also showed that both variants lead to the production of aberrant transcripts affecting *OTUD6B* splicing with experimentally validated findings that c.324+1G >C causes the complete skipping of exon 2 that leads to a frameshift (p.Ala58Aspfs_6). Among the variants described by Santiago-Sim et al. (2017) all affect both protein isoforms including the OTU domain, except for 1 splicing variation (c.173–2A>G) in family 5 that could lead to the production of an intact OTUD6B-2 protein with the skipping of exon 2. They did not, however, report experimental validation findings for the c.173–2A>G variation on splicing in patients with the mild or moderate phenotype (Santiago-Sim et al., 2017). These findings may explain the phenotypic differences in the clinical severity of the cases with splice site variants. An additional 4 variants have been described in the two most recent publications. Two of them were discovered in two unrelated families by Abdel-Salam et al. (2022); 1 homozygous nonsense variant (NM_016023.3:c.271C>T) (p.Gln91*) in exon 2 and homozygous missense variant (NM_016023.3:c.767G>T) (p.Gly256Val) in exon 5. Phetthong et al. (2021) described compound heterozygous frameshift variant and 0.118 Mb deletion of 8q21.3, chr8:92084087-92202189, with OTUD6B involved.

In all, four of the previously described variants and one of the novel variants in the presented case are located in exon 4, and the 3 previously described variants are located in the intron (1, 2, and 3) splice site of *OTUD6B* (Table 1). The OTUD6B protein includes 3 coiled-coil domains (CC) and an OTU-like cysteine protease domain [18]. Specially, cases carrying the variants that changed the OTU-domain had the severe clinical phenotype, except for those with p.Tyr216Cys and p.Gly256Val. In addition, it is remarkable that the variants are clustered in exon 4 and truncated. In the present study, when the approximate location of the amino acid changes in the OTUD6B protein was examined both variants seemed to have

a potential effect on the amino acid sequence of the only OTU domain of the OTUD6B protein that is a key functional domain. The novel likely gene-disruptive (LGD) variant [(NM_016023.3:c.617_618del) (NP_057107.4:p.Val206Glyfs*9)] in exon 4 of *OTUD6B* in the presented case was predicted to undergo degradation via nonsense-mediated decay (NMD+) of the mRNA molecule. This frameshift variant was performed by an indel of nucleotides between the highly conserved residue cysteine loop (C-loop) and variable loop into the OTU domain of OTUD6B (Fig. 3B, D). The shift site in the OTU domain did not include the cysteine loop, but did include the H-loop and variable loop from the locations of the conserved predicted ubiquitin binding sites within the OTU domain (Fig. 3B).

The present study also described an additional novel missense variant [(NM_016023.3:c.821 T>G) (NP_057107.4:p.Ile274Arg)] located in exon 6 that leads to an amino acid change (isoleucine to arginine) between the highly conserved residue histidine loop (H-loop) and variable loop into the OTU domain of OTUD6B (Fig. 3B, D). *In silico* analysis of the novel p.Ile274Arg variant suggested that this variant was rare and predicted to be pathogenic (Supplementary Table 1).

The severe clinical phenotype of the intellectual developmental syndrome in the presented case might be indicative of the functional importance of the region in the OTU domain, including the variants. In particular, the region affected by the missense variants may be important for defining specific additional residues with protease activity and cleavage specificity. At the same time, the first missense variant (p.Tyr216Cys) that is between the C-loop and variable loop into the OTU domain of OTUD6B first described by Santiago-Sim et al. (2017) was hypomorphic and associated with a less severe phenotype, suggesting it may not be important (suitable) to evaluate its regional functionality in the OTU domain, whereas the presented patient with the novel missense variant had the severe phenotype.

The two novel variants in *OTUD6B* reported herein will most likely prove to be important for understanding the relationship of protein deubiquitination to intellectual developmental syndromes. DUBs have an essential role in regulating DNA repair, protein degradation, apoptosis and immune response. The importance of proper regulation of protein deubiquitination is indicated by the identification of variants in DUB genes in such diseases as cancer and neurodegeneration (Clague et al., 2013); therefore, rare pathogenic variants are important for understanding the function and regulation of the genes. When the previously reported patients and the presented patient carrying the variants in *OTUD6B* were evaluated according to the genetic and clinical features, the severity of the phenotype of the patients with *OTUD6B* gene variant differed.

The patients shown in Table 1 presented with dysmorphic features, epilepsy, spasticity, and extremity abnormalities. Case 3-18 and the presented case have very severe clinical features, including severe intellectual disability, structural brain malformation, microcephaly, absence of speech, inability to walk, hypotonia, feeding problems, congenital heart defect, and generalized tonic-clonic seizures, whereas case 2, 19, 20, 21 have a less severe clinical phenotype, with mild to moderate intellectual disability, but normal speech and motor development (Table 1). The presented patient had a similar phenotype as the previously reported patients with *OTUD6B* variants in family 1-5 described by Santiago-Sim et al.

(2017) and case 15, 16, 17 (Alkuraya et al., 2020; Abdel-Salam et al., 2022) (Table 1). The presented case has also similar common phenotypic features including characteristic facial dysmorphology and hand pattern including clubbed fingers with broad thumbs in Patient II.2 (Figure1/O; Figure 2/G, H) reported by Abdel-Salam et al. (2022).

Interestingly, cranial MRI in the index case showed partial agenesis of the corpus callosum (pACC) characterized by the absence of some its parts. ACC might occur together with other malformations that lead to the syndrome and are present in 1-3% of cases with the impaired neurodevelopment (Hofman et al., 2020). A single MRI image showing partial or short corpus callosum agenesis was also noted in individual II-4 from family 3, including the LGD variant (p.Arg145*) reported by Santiago-Sim et al. (2017) (Supplementary Figure 1). To show the similarity in corpus callosum abnormalities, the present study compared MRI sagittal images of the brain indicating partial agenesis of the corpus callosum in the present and previously reported cases (II-4 from family 3) with *OTUD6B* variants (Supplementary Figure 1). Although the findings suggest that pACC might be a specific feature of the severe IDDFSDA phenotype associated with *OTUD6B* variants; however, additional functional studies are required and other novel variants need to be detected, so as to more fully delineate the phenotypic spectrum of the variants in *OTUD6B* and to more clearly understand the mechanism of normal ACC development. Although the missense variant (p.Tyr216Cys) in exon 4 and maps to the same OTU domain in family 6 (Fig. 3B, D) that was predicted to be deleterious via *in silico* tools (Supplementary Table 1), the phenotype of the patient was less severe, as compared to the patients (including the presented patient) with truncating *OTUD6B* variants.

The phenotypic severity depends on the residual protein function of the sum of two alleles in an autosomal recessive disorder. To predict the relationship between genotype and phenotypic severity, the effects of the missense variants [(NM_016023.3:c.821 T>G) (NP_057107.4:p.Ile274Arg)] on the other allele and on the structure and function of the OTUD6B protein was further investigated together with a previously reported first homozygous missense variant (p.Tyr216Cys) in the same domain in a patient with a less severe IDDFSDA phenotype.

In the further investigations, the 3D structure of OTUD6B was modeled; the obtained structures and variants locations within the catalytic triad are given in Figure 4. The stability changes for Tyr216Cys and Ile274Arg are predicted, indicating that both substitutions cause instability in the OTU domain, although Ile274Arg substitution leads to a more significant drastic change in stability. When we simulated the Ile274-Arg variant protein, we could never obtain a stable structure. As such, it was hypothesized that Tyr216Cys will lead to localized destabilization, whereas Ile274Arg will lead to significant distortion in the overall fold of OTUD6B. These results explained why cases from family 6 reported by Santiago-Sim et al. (2017) had a less severe disease phenotype than the presented patient (Table 1).

In conclusion, our findings support that the clinical severity could be related with the predicted functional severity of the variations in OTUD6B. The findings confirm that IDDFSD—with its wide phenotypic spectrum —can be classified as 2 types: severe and less

severe. Moreover, the severe clinical phenotype of the intellectual developmental syndrome in the presented case might be indicative of the functional importance of the region in the OTU domain, including the variants. The clinical phenotype severity predicting by genomic variations could simplify diagnosis and therapy. However, additional functional studies are required.

Supplementary Material

Refer to Web version on PubMed Central for supplementary material.

Acknowledgements

We are very grateful to the families that participated in this study.

Funding

This work was supported in part by Grant given to SC Scientific and Technological Research Council of Turkey (TÜBİTAK-BIDEB 2219) (International Postdoctoral Research Scholarship Programme) and a grant from the US National Institutes of Health (NIH R01 MH101221 to E.E.E). Sequencing was provided by the University of Washington Center for Mendelian Genomics (UW-CMG) and was funded by NHGRI and NHLBI grants HG006493 and U24 HG008956. The content is solely the responsibility of the authers and does not necessarily represent the official views of the National Institutes of Health. This work has been supported with the Dokuz Eylul University Fund (2018.KB.SAG.116), The Scientific and Technological Research Council of Turkey (TÜBİTAK) (106S099) and the EMBO Installation Grant (Project # 4421).

References

Abdel-Salam GM, Abdel-Hamid MS, Sayed IS, Zechner U, Bolz HJ, 2022. OTUD6B-associated intellectual disability: Novel variants and genetic exclusion of retinal degeneration as part of a refined phenotype. J. Hum. Genet 67, 55–64. 10.1038/s10038-021-00966-2 [PubMed: 34354232]

Abraham MJ, Murtola T, Schulz R, Páll S, Smith JC, Hess B, Lindahl E, 2015. GROMACS: High performance molecular simulations through multi-level parallelism from laptops to supercomputers. SoftwareX. 1, 19–25. 10.1016/j.softx.2015.06.001

Alkuraya FS, 2020. Phenotypic expansion of OTUD6B-related syndrome. Am. J. Med. Genet. A 182, 1530–1531. 10.1002/ajmg.a.61548 [PubMed: 32181568]

Clague MJ, Barsukov I, Coulson JM, Liu H, Rigden DJ, Urbe S, 2013. Deubiquitylases from genes to organism. Physiol. Rev 93, 1289–315. 10.1152/physrev.00002.2013 [PubMed: 23899565]

Hofman J, Hutny M, Sztuba K, Paprocka J, 2020. Corpus callosum agenesis: An insight into the etiology and spectrum of symptoms. Brain Sci. 10, 625. 10.3390/brainsci10090625

Kayagaki N, Phung Q, Chan S, Chaudhari R, Quan C, O'Rourke KM, Eby M, Pietras E, Cheng G, Bazan JF, Zhang Z, Arnott D, Dixit VM, 2007. A deubiquitinase that regulates type I interferon production. Science. 318, 1628–1632. 10.1126/science.1145918 [PubMed: 17991829]

Komander D, Barford D, 2008. Structure of the A20 OTU domain and mechanistic insights into deubiquitination. Biochem. J 409, 77–85. 10.1042/BJ20071399 [PubMed: 17961127]

Komander D, Clague MJ, Urbe S, 2009. Breaking the chains: structure and function of the deubiquitinases. Nat. Rev. Mol. Cell Biol 10, 550–63. 10.1038/nrm2731 [PubMed: 19626045]

Laimer J, Hofer H, Fritz M, Wegenkittl S, Lackner P, 2015. MAESTRO-multi agent stability prediction upon point mutations. BMC Bioinformatics. 16, 116. 10.1186/s12859-015-0548-6 [PubMed: 25885774]

Landau M, Mayrose I, Rosenberg Y, Glaser F, Martz E, Pupko T, Ben-Tal N, 2005. ConSurf 2005: the projection of evolutionary conservation scores of residues on protein structures. Nucl. Acids Res 33, W299–W302. 10.1093/nar/gki370 [PubMed: 15980475]

Matthijs G, Souche E, Alders M, Corveleyn A, Eck S, Feenstra I, Race V, Sistermans E, Sturm M, Weiss M, Yntema H, Bakker E, Scheffer H, Bauer P, 2016. Guidelines for diagnostic next-generation sequencing. Eur. J. Hum. Genet 24, 2–5. 10.1038/ejhg.2015.226 [PubMed: 26508566]

Mevissen TE, Hospenthal MK, Geurink PP, Elliott PR, Akutsu M, Arnaudo N, Ekkebus R, Kulathu Y, Wauer T, El Oualid F, Freund SMV, Ovaa H, Komander D, 2013. OTU deubiquitinases reveal mechanisms of linkage specificity and enable ubiquitin chain restriction analysis. Cell. 154, 169–184. 10.1016/j.cell.2013.05.046 [PubMed: 23827681]

Phetthong T, Khongkrapan A, Jinawath N, Seo GH, Wattanasirichaigoon D, 2021. Compound heterozygote of point mutation and chromosomal Microdeletion involving OTUD6B coinciding with ZMIZ1 variant in syndromic intellectual disability. Genes. 12, 1583. 10.3390/genes12101583 [PubMed: 34680978]

Pires DE, Ascher DB, Blundell TL, 2014. DUET: a server for predicting effects of mutations on protein stability using an integrated computational approach. Nucleic Acids Res. 42, W314–W319. 10.1093/nar/gku411 [PubMed: 24829462]

Richards S, Aziz N, Bale S, Bick D, Das S, Gastier-Foster J, Grody WW, Hegde M, Lyon E, Spector E, Voelkerding K, Rehm HL, 2015. Standards and guidelines for the interpretation of sequence variants: a joint consensus recommendation of the American College of Medical Genetics and Genomics and the Association for Molecular Pathology. Genet. Med 17, 405–24. 10.1038/gim.2015.30 [PubMed: 25741868]

Rump P, Jazayeri O, van Dijk-Bos KK, Johansson LF, van Essen AJ, Verheji JBGM, Veenstra-Knol HE, Redeker EJW, Mannens MMAM, Swertz MA, Alizadeh BZ, van Ravenswaaij-Arts CMA, Sinke RJ, Sikkema-Raddatz B, 2015. Whole-exome sequencing is a powerful approach for establishing the etiological diagnosis in patients with intellectual disability and microcephaly. BMC Med. Genomics 9, 7. 10.1186/s12920-016-0167-8

Santiago-Sim T, Burrage LC, Ebstein F, Tokita MJ, Miller M, Bi W, Braxton AA, Rosenfeld JA, Shahrour M, Lehmann A, Cogné B, Küry S, Besnard T, Isidor B, Bézieau S, Hazart I, Nagakura H, Immken LL, Littlejohn RO, Roeder E, Afawi Z, Balling R, Barisic N, Baulac S, Craiu D, De Jonghe P, Guerrero-Lopez R, Guerrini R, Helbig I, Hjalgrim H, Jähn J, Klein KM, Leguern E, Lerche H, Marini C, Muhle H, Rosenow F, Serratosa J, Sterbová K, Suls A, Moller RS, Striano P, Weber Y, Zara F, Kara B, Hardies K, Weckhuysen S, May P, Lemke JR, Elpeleg O, Abu-Libdeh B, James KN, Silhavy JL, Issa MY, Zaki MS, Gleeson JG, Seavitt JR, Dickinson ME, Ljungberg MC, Wells S, Johnson SJ, Teboul L, Eng CM, Yang Y, Kloetzel P-M, Heaney JD, M.A. Walkiewicz, 2017. Biallelic variants in OTUD6B cause an intellectual disability syndrome associated with seizures and dysmorphic features. Am. J. Hum. Genet 100, 676–688. 10.1016/j.ajhg.2017.03.001 [PubMed: 28343629]

Straniero L, Rimoldi V, Soldà G, Bellini M, Biasucci G, Asselta R, Duga S, 2018. First replication of the involvement of OTUD6B in intellectual disability syndrome with seizures and dysmorphic features. Front. Genet 9, 464. 10.3389/fgene.2018.00464 [PubMed: 30364145]

Webb B, Sali A, 2016. Comparative protein structure modeling using modeller. Current Protocols in Bioinformatics 54, John Wiley & Sons, Inc., 5.6.1–5.6.37. 10.1002/cpbi.3 [PubMed: 27322406]

Xu Z, Zheng Y, Zhu Y, Kong X, Hu L, 2011. Evidence for OTUD-6B participation in B lymphocytes cell cycle after cytokine stimulation. PLoS One. 6, e14514. 10.1371/journal.pone.0014514 [PubMed: 21267069]

Zimmermann L, Stephens A, Nam SZ, Rau D, Kübler J, Lozajic M, Gabler F, Söding J, Lupas AN, Alva V, 2018. A completely reimplemented MPI bioinformatics toolkit with a new HHpred server at its core. J. Mol. Biol 430, 2237–2243. 10.1016/j.jmb.2017.12.007 [PubMed: 29258817]

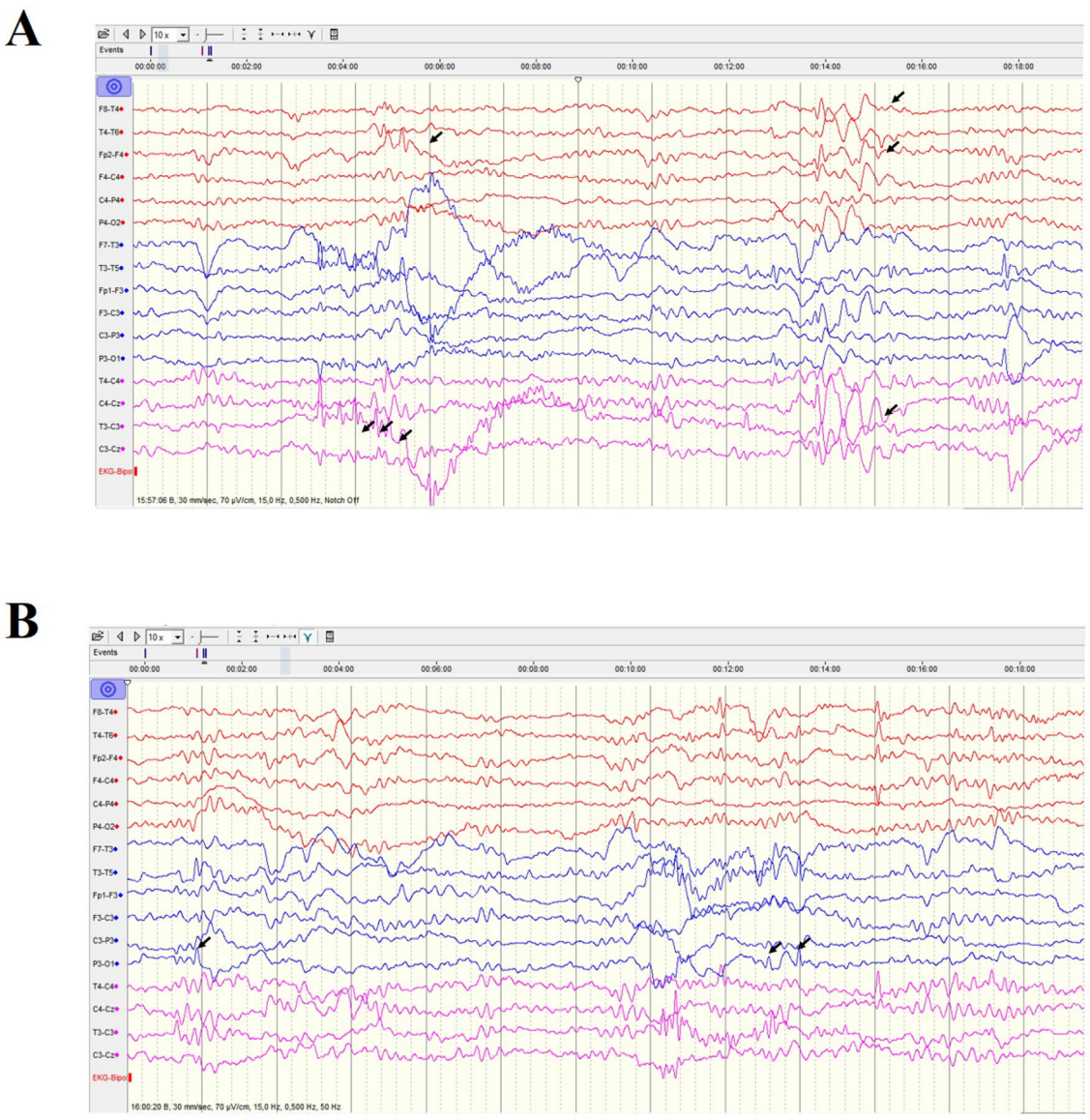

Figure 1.

EEG shows asynchronous multifocal epileptic discharges originating from both hemispheres. [2- 4 Hz centrotemporal spikes (T3-C3) and right frontal sharp-slow wave discharges (F2-F4) in Figure 1A, left parietooccipital sharp waves in Figure 1B marked by black arrows, predominantly seen on bipolar montage EEG].

Figure 2.

A. Dysmorphological facial features of the presented patient including hypotelorism, long-arched and sparse eyebrows, prominent and beaked nose, high arched palate and midfacial hypoplasia large ears with hypo plastic helical crimp, long philtrum, and thin upper lip, and severe scoliosis (including left thorasic hump and pelvic obliquity with chest deformity called pectus carinatum) **B.** Bilateral planovalgus deformity with overlapping toes.

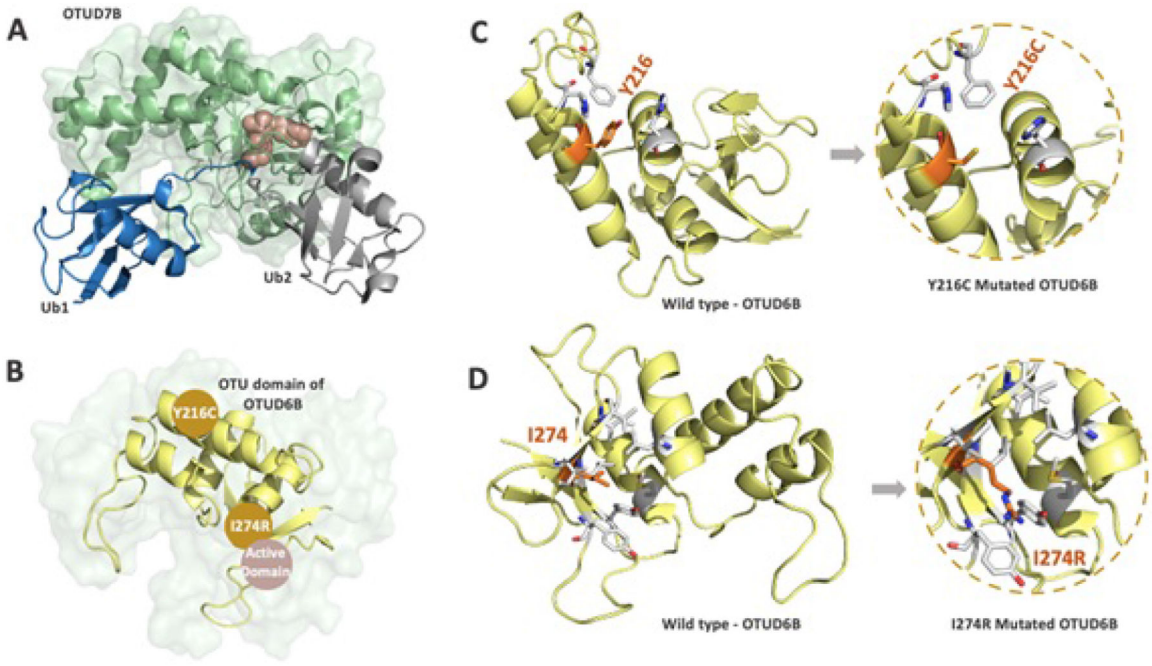

Figure 3.

A. Pedigree for the reported family. Black symbol, squares, and circles represent the index case, males, and females, respectively. **B.** Schematic representation of the protein encoded by the gene *OTUD6B* (NM_016023.3; GRCh37/hg19). The variants reported herein are shown in framed. **c.** Conservation analysis illustrates a high level of conservation of Ile274. d. Genomic locations of the variants reported within *OTUD6B*. The variants reported herein are shown in framed. The missense variant [(NM_016023.3:c.821T>G) (NP_057107.4:p.Ile274Arg)] was not reported in gnomAD. The maximum subpopulation allele frequency (maxAAF) of the frameshift variant [(NM_016023.3:c.617_618del) (NP_057107.4:p.Val206Glyfs*9)] was 0.000008314 (2/240562 alleles) in gnomAD. A homozygous state was not detected in gnomAD.

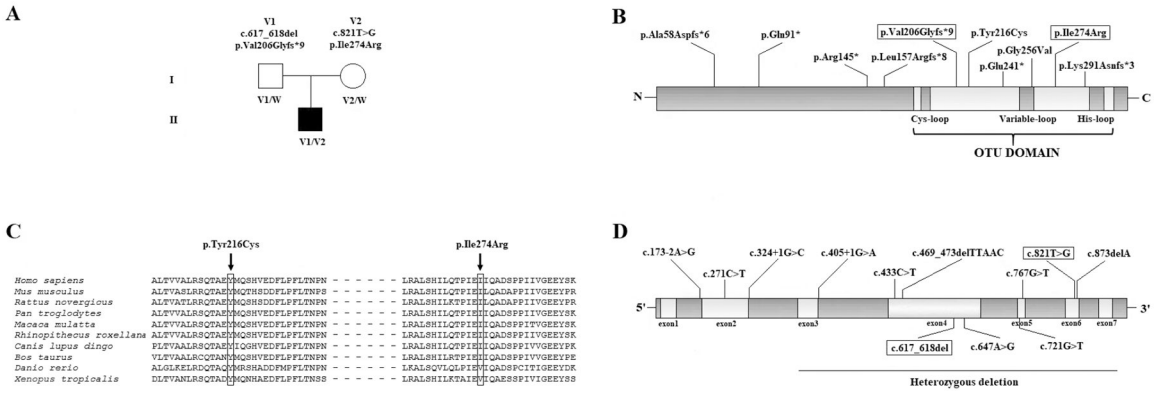

Figure 4.

A. The crystal structure of Cezanne/OTUD7B in complex with the di-Ub chain. OTUD7B is depicted in pale green cartoon/surface, bound to a di-ubiquitin chain (blue and gray) (PDB ID: 5LRV). The catalytic triad of the OTU domain is shown with pink spheres. **B.** The model of human OTUD6B's OTU domain. The two-point variant locations, Tyr216Cys and Ile274Arg, are noted with orange circles and the catalytic triad is noted with a pink circle. The distance between the catalytic triad and the 216th position is >20 Å and the distance between the catalytic triad and the 274th position is ~8 Å. **C.** The wild-type model of OTUD6B; Tyr216's (orange sticks) important surrounding amino acids (gray sticks) are highlighted. In the wild-type form, TYR216 is surrounded by aromatic amino acids, leading to an aromatic packing that will be lost in the case of Tyr216Cys (right encircled panel). **D.** The wild-type model of OTUD6B; I274's (orange sticks) important surrounding amino acids (gray sticks) are highlighted. In the wild-type form, ILE 274 is surrounded by hydrophobic amino acids, leading to a hydrophobic core that will be highly destabilized upon Ile274Arg variant, as depicted by the circled panel.

Table 1.

of patients carrying *OTUD6B* variants.

Current Study	Straniero et al, 2018	Santiago et al, 2017	Santiago et al, 2017	Santiago et al, 2017	Santiago et al, 2017	Santiago et al, 2017	Santiago et al, 2017	Santiago et al, 2017	Santiago et al, 2017
1	2	3 / F1	4 / F2	5 / F3 / S2	6 / F3 / S4	7 / F3 / S5	8 /F4 / S3	9 /F4 / S4	10 / F5 / S1
Male	Female	Female	Male	Male	Male	Male	Male	Male	Female
17 years	6 years	18 years 2 months	17 years 2 months	13 years/Ex	8 years 1 month	3 years	9 years 5 months	3 years 11 months	5 years 4 months
Turkey	Italy	Hispanic	Hispanic /Italy	Egypt	Egypt	Egypt	Syria	Syria	Palestine
(−)	(−)	(−)	(−)	yes	yes	yes	yes	yes	yes
PM (32 g.w.) SGA	IUGR	IUGR	IUGR, oligohydramniosis and poor fetal activity	IUGR	IUGR	IUGR	IUGR	IUGR	(−)
pp:15 months walk:3 years	sit unsupp:11 months walk:18 months	sit unsupp:9 months walk:18 months	sit unsupp:18 months walk:3 years 9 months	only sits independently never walks	only sits non-ambulatory	not able to sit non-ambulatory	sit unsupp:NA, walk: 4 years 6 months,	sit unsupp: NA, never walks	unsup.sit:24 months, walk: 5 years
Non-ambu.	Ambu	Ambu(partially)	Non-ambu.	Non-ambu.	Non-ambu.	Non-ambu.	Ambu	Non-ambu.	Ambu(partially)
(+) / severe	(+) / mild - moderate	(+) / severe	(+) / severe	(+) / severe	(+) / severe	(+) / severe	(+) / severe	(+) / severe	(+) / severe
no words	first words at 2 years	no words	no words	no words	no words	no words	no words	no words	only sounds
(−)	episodic behavioral disorders	(−)	(−)	autistic features	autistic features	autistic features	(−)	(−)	(−)
yes	yes	yes	yes	yes	yes	yes	yes	yes	yes
GTC	GTC	*	GTC, behavioral arrest	GTC	NA	NA	NA	NA (only one attack)	myoclonic
8 months	5 years	12 months	15 months	NA	NA	NA	17 months	3 years	7 months
PB, VPA, LEV	VPA	NA	+ VNS	NA	NA	NA	NA	NA	NA
partial	NA	Refractory	Refractory	NA	NA	NA	NA	self-limted	Refractory
al centro-temporoparietal sharp waves	NA	NA	NA	NA	NA	NA	NA	NA	NA
halamic encephalomalasia corpus callosum (rostral agenesis)	Normal	Normal	prominent perivascular spaces, CCH leucodystrophy	mild frontoparietal cortical changes	mild frontoparietal cortical changes CCH	mild frontoparietal cortical changes	Normal	cerebral atrophy (both cortical and white matter)	mild LV dilatation CCH

Current Study	Straniero et al, 2018	Santiago et al, 2017	Santiago et al, 2017	Santiago et al, 2017	Santiago et al, 2017	Santiago et al, 2017	Santiago et al, 2017	Santiago et al, 2017	Santiago et al, 2017
yes	yes	yes	yes	yes	yes	yes	yes	yes	yes
ehead, long face sparse hair	High forehead long face	displaced posterior hair whorl	sparse hair	short neck sloping shoulders	short neck sloping shoulders	short neck sloping shoulders	(−)	(−)	sparse hair flat occiput
ched and sparse eyebrows elashes, hypotelorism, deep t eyes, bilateral ptosis	sunken eyes and hypotelorism	long arched eyebrows long eyelashes long palpebral fissures	full arched eyebrows, mild ptosis	long palpebral fissures	long palpebral fissures	long palpebral fissures	long palpebral fissures	(−)	full arched eyebrows deep set eyes long eyelashes
protruding and posteriorly ears with hypoplasic helical crimp	large protruding ears	(−)	posterior rotated ears with bilateral pits	large protruding and low set ears	large protruding and low set ears	large protruding and low set ears	large ears	large ears	large ears
d and prominent nasal antevert nostrils long and bulbous nose	hanging columella	long nose,hypoplasitc alae high nasal bridge	long nose with prominent nasal bridge	broad and prominent nasal bridge	broad and prominent nasal bridge	broad and prominent nasal bridge	(−)	(−)	(−)
g philtrum thin upper p, high arched palate rominent chin,retrognatia akrodontia,crowding	long philtrum thin upper lip high arched palate retrognatia	long philtrum high arched palate mild retrognatia	long philtrum,thin upper lip and high arched palate with retrognatia	long philtrum thin upper lip retrognatia	long philtrum thin upper lip retrognatia	long philtrum thin upper lip retrognatia	(−)	(−)	long philtrum thin upper lip
yes	yes	yes	yes	yes	yes	yes	yes	yes	yes
ypotonia limb hypertonia	(−)	generalised hypotonia	axial hypotonia limb hypertonia	generalised hypotonia	generalised hypotonia	generalised hypotonia	generalised hypotonia	generalised hypotonia	generalised hypotonia
brisk	NA	NA	NA	NA	NA	NA	NA	NA	NA
yes	(−)	yes	yes	NA	NA	NA	NA	NA	NA
(−)	(−)	ataxia	ataxia	NA	NA	NA	NA	NA	NA
tracheostomized	(−)	tracheostomized	OSAS (with partial ventilator dependence) Asthma	recurrent pneumonia	NA	NA	NA	NA	NA
TEF	TEF	(−)	(−)	PS, ASD	(−)	PS, ASD, VSD	NA	IVSD	(−)
Yes	(−)	yes	yes	yes	yes	yes	yes	yes	(−)

Eur J Med Genet. Author manuscript; available in PMC 2023 June 01.

Current Study		Straniero et al, 2018		Santiago et al, 2017	Santiago et al, 2017	Santiago et al, 2017	Santiago et al, 2017	Santiago et al, 2017	Santiago et al, 2017	Santiago et al, 2017	Santiago et al, 2017
Yes		GER(acquired)		GER(acquired)	yes	yes	NA	NA	yes	yes	yes
PEG		(−)		PEG	PEG	(−)	NA	NA	NA	PEG	(−)
pe kidneys, inguinal hernia		(−)		(−)	RTA neurogenic bladder bilateral retractile testes	(−)	cryptorchidism	(−)	cryptorchidism	bilateral cryptorchidism	(−)
(+) / severe		(−)		severe kyphoscoliosis	(+) / severe	(+) / NA	(−)	(−)	(−)	(+) / NA	(+) / NA
:arachnodactyly,clubbed ers, elbow hyperlaxity distal phalangae (thumb alluces) lower:overriding allux valgus,planovalgus		Upper:broad thumbs, fetal pads. Lower:overriding toes		Upper: broad thumbs, tapered fingers Lower: brachydactyly of toes and hallux valgus	Upper:broad thumbs bulbous finger tips. Lower: overriding toes planovalgus	Upper:broad thumbs clubbed fingers. Lower:clubfoot	Upper:broad thumbs interphalangeal hyperlaxity. Lower:overriding toes	Upper:broad thumbs interphalangeal hyperlaxity. Lower:overriding toes	Upper:broad thumbs fetal pads. Lower:broad first toes	(−)	Upper:-Lower: bilateral syndactyly of toes
pectus carinatum		(−)		(−)	(−)	(−)	(−)	(−)	(−)	(−)	(−)
ion contractures(knee)		NA		yes	yes	(−)	(−)	(−)	(−)	(−)	(−)
(−)		(−)		hypothyroidism bilateral hearing loss	sensorineural hearing loss GH deficency HGG	(−)	(−)	(−)	retinopathy with abnormal ERG	hypothyroidism short stature	(−)
577530	(−)	rs767665903	rs751309307	rs368313959	rs368313959	rs368313959	rs368313959	rs368313959	rs759317757	rs759317757	rs1064797102
618del	c.821T>G	c.324+1G>C	c.405+1G>A	c.433C>T	c.433C>T	c.433C>T	c.433C>T	c.433C>T	c.469_473delTTAAC	c.469_473delTTAAC	c.173–2A>G
Glyfs*9	p.Ile274Argfs*3	p.Ala58Aspfs*6	-	p.Arg145*	p.Arg145*	p.Arg145*	p.Arg145*	p.Arg145*	p.Leu157Argfs*8	p.Leu157Argfs*8	(−)
n 4	exon 6	intron 2	intron 3	exon 4	exon 4	exon 4	exon 4	exon 4	exon 4	exon 4	intron 1
0008	(−)	0.000004	-	0.00015	0.00015	0.00015	0.00015	0.00015	(−)	(−)	(−)
rnal	maternal	paternal	maternal	NA	NA	NA	NA	NA	NA	NA	NA
go et al, 17	**Santiago et al, 2017**	**Santiago et al, 2017**	**Santiago et al, 2017**	**Alkuraya et al, 2020**	**Abdel-Salam et al, 2021**	**Abdel-Salam et al, 2021**	**Abdel-Salam et al, 2021**	**Abdel-Salam et al, 2021**	**Abdel-Salam et al, 2021**	**Phetthong et al, 2021**	
5 / S2	12 /F6 / S1	13 / F6 / S2	14 / F6 / S3	15	16 /F1/S1	17 /F1/S2	18 /F2/S1	19 /F2/S2	20 /F2/S3	21	
nale	Male	Male	Female	Female	Male	Male	Male	Female	Female	Female	
2 months	20 years 7 months	16 years 6 months	14 years 8 months	10 months	9 years	7 years	11 years	6 years	24 Years	5 years	
stine	Turkey	Turkey	Turkey	NA	Egyptian	Egyptian	Egyptian	Egyptian	Egyptian	South East Asia	

Eur J Med Genet. Author manuscript; available in PMC 2023 June 01.

Current Study		Straniero et al, 2018		Santiago et al, 2017	Santiago et al, 2017	Santiago et al, 2017	Santiago et al, 2017	Santiago et al, 2017	Santiago et al, 2017	Santiago et al, 2017	Santiago et al, 2017
es	yes	yes	yes	yes	Yes	yes	yes	yes	yes	-	
-)	(−)	(−)	(−)	IUGR, oligohydramnios	congenital hypotonia (NICU for 2 months)	IUGR (NICU for 17 days,poor sucking)	IUGR (NICU for 9 days,poor sucking)	IUGR	NA	prematurity (37 g.w.) SGA	
e to sit	Normal	Normal	Normal	unable to sit	head control: 18 months sit unsupp: 3 years walk supp:8 years	head control: 6 months sit supp: 16 months walk : 3 years	sit unsupp: 18 months walk : 30 months	sit unsupp: 12 months walk :24 months	walk :3 ½ years	Hold to stand: 18 months Walk:: 3years 6 months	
ambu	Ambu	Ambu	Ambu	Non-ambu	Ambu (partially)	NA	Ambu (partially,waddling gait)	NA	NA	Ambu	
evere	(+) / moderate	(+) / mild	(+) / moderate	(+) / severe	(+) / severe	(+) / severe	(+) / severe	(+) / moderate	(+) / moderate	(+) / moderate	
ords	(−)	(−)	(−)	no words	no words	no words	no words	few words	few words, severe	few words	
-)	learning difficulty (early childhood)	(−)	(−)	(−)	autistic features self-mutilation	autistic features self-mutilation	autistic features self-mutilation	autistic features hand stereotipies	NA		
es	yes	yes	yes	(−)	yes	yes	yes	(−)	NA	yes	
A	febrile seizures,GTC	NA	NA	(−)	GTC	GTC	GTC	febrile seizures only	NA	febrile seizure(12-24 months) GTC and atonic seizures	
ears	18 months	7 years	8 years	(−)	3 months	3 months	8 months	NA	6 months	28-29 months	
A	NA	NA	NA	(−)	CBZ, VPA, LEV, CZP	CBZ, VPA	VPA, LEV	NA	VPA	PB,VPA,TPM	
A	NA	NA	NA	(−)	refractory	yes	yes	(−)	NA	refractory	
A	NA	NA	NA	(−)	slow background activity with delta-teta waves	NA	generalised epileptic discharges (no additional data)	Normal	NA	NA	
mal	Normal	Normal	Normal	Normal	mild asymmetric ventriculomegaly delayed myelination CCH cerebellar vermiş atrophy	CCH	prominent perivascular spaces delayed myelination	Normal	NA	NA	

Eur J Med Genet. Author manuscript; available in PMC 2023 June 01.

Current Study		Straniero et al, 2018		Santiago et al, 2017	Santiago et al, 2017	Santiago et al, 2017	Santiago et al, 2017	Santiago et al, 2017	Santiago et al, 2017	Santiago et al, 2017	Santiago et al, 2017
es	yes	yes	yes	yes	yes	yes	yes	yes	yes	yes	
cciput	narrow long face with wide forehead prominent facial asymmetry	narrow long face with wide forehead	narrow long face wrth wide forehead	scant scalp hair plagiocephaly	high forehead, long face sparse hair	high forehead, long face sparse hair	long face, sparse hair	long face high forehead, sparse hair	long face high forehead	Coarse face with hanging cheek	
et eyes long shes	down-slating palpebral fissures	(−)	(−)	epicanthus, entropion right ptosis, long eyelashes,	sparse eyebrows, convergent squint partial ptosis	sparse eyebrows partial ptosis	double-arched eyebrows bilateral ptosis	sparse eyebrows bilateral ptosis	sparse outer eyebrows narrow palpebral fissures partial ptosis	Arched and sparse outer eyebrows	
ears	dysplastic anterior-angled ears	(−)	(−)	hypoplastic antihelix with cupped ear appearance	low-set ears	low-set posteriorly rotated ears	Cup-shaped ears	Low set large ears	large low set ears		
−)	tubular nose	(−)	(−)	bulbous nose	long nose anteverted nostrils	long nose anteverted nostrils	long nose anteverted nostrils	Long nose, anteverted nostrils	long nose anteverted nostrils	Prominent nasal bridge	
hiltrum per lip	high arched palate malocclusion of teeth	high arched palate	high arched palate	long philtrum, thin upper lip, midline tongue furrow mild micronathia	Long and flat philtrum Tented upper lip Macrodontia crowding, partial ankyloglossia bifid tip of the tongue,	long philtrum macrodontia, crowding, partial ankyloglossia, high- arched palate	Long broad philtrum, partial ankyloglossia, everted lips, high-arched palate,long uvula, macrodontia, crowding	long flat philtrum, long pointed chin partial ankyloglossia, crowding	long flat philtrum macrodontia, crowding, macrostomia	long philtrum thin upper lip	
es	(−)	(−)	(−)	yes	yes(borderline)	yes	yes	yes(borderline)	NA	(−)	
alised tonia	NA	NA	NA	axial and appendicular hypertonia	limb hypertonia	NA	NA	generalised hypotonia	NA	Normal	
A	NA	NA	NA	NA	brisk	NA	NA	normoactive	NA	normoactive	
A	NA	NA	NA	yes	NA	NA	NA	NA	NA	(−)	
A	NA	NA	NA	(−)	NA	NA	NA	NA	NA	NA	
A	NA	NA	NA	frequent pulmonary infections	NA	NA	NA	NA	NA	NA	
cundum SD	NA	NA	NA	RVH,PS	(−)	(−)	VSD	(−)	NA	ASD,VSD,PS	

Eur J Med Genet. Author manuscript; available in PMC 2023 June 01.

Current Study		Straniero et al, 2018		Santiago et al, 2017	Santiago et al, 2017	Santiago et al, 2017	Santiago et al, 2017	Santiago et al, 2017	Santiago et al, 2017	Santiago et al, 2017	Santiago et al, 2017
-)	(−)	(−)	(−)	(+) /severe	(+)	(+)	(+)	(+)	NA	(−)	
es	(−)	(−)	(−)	pharyngeal dysphagia GERD pylor stenosis	NA	NA	NA	NA	NA	(−)	
-)	(−)	(−)	(−)	NA	NA	NA	NA	NA	NA	(−)	
-)	(−)	(−)	(−)	left cortical renal cyst	bilateral undescended testicles	bilateral undescended Testicles large umbilical and inguinal hernia(infancy)	(−)	NA	NA	(−)	
-)	(−)	(−)	(−)	(+) / severe	NA		(+) / kyphoscoliosis	NA	NA	NA	
er (−) bilateral tyly of es	arachnodactyly	elbow hyperlaxity	elbow hyperlaxity, arachnodactyly	right hand and left foot post axial polydactyly	fetal pads, broad distal phalanges (thumbs and halluces) prominent interphalangeal joints	broad distal phalanges (thumbs and halluces)	fetal pads, broad distal phalanges (thumbs and halluces) prominent interphalangeal joints	fetal pads, broad distal phalanges (thumbs and halluces) prominent interphalangeal joints	broad distal phalanges (thumbs and halluces) prominent interphalangeal joints	Left hand postaxial polydactyly broad distal phalangae (thumbs and halluces)	
-)	(−)	(−)	(−)	(−)	NA	NA	pectus carinatum	NA	NA	NA	
-)	(−)	(−)	(−)	NA	NA	NA	NA	NA	NA	NA	
				left developmental hip dysplasia butterfly vertebra (T8)	hearing loss (recurrent otitis media) optic atrophy choriaretinal degeneration	optic atrophy choriaretinal degeneration	pilonidal sinus			Tight heel cord	
97102	rs1064797103	rs1064797103	rs1064797103	rs772032719	-	-	-	-	-	rs762934606	-
A>G	c.647A>G	c.647A>G	c.647A>G	c.721G>T	c.271C>T	c.271C>T	c.767G>T	c.767G>T	c.767G>T	c.873delA	-
	p.Tyr216Cys	p.Tyr216Cys	p.Tyr216Cys	p.Glu241*	p.Gln91*	p.Gln91*	p.Gly256Val	p.Gly256Val	p.Gly256Val	p.Lys291asnfs*3	DEL
	exon 4	exon 4	exon 4	exon 5	exon 2	exon 2	exon 5	exon 5	exon 5	exon 6	exon 3-7
	-	-	-	-	-	-	-	-	-	0.00003926	3 cases in DECIPHER
	NA	NA	NA	NA	NA	NA	NA	NA	NA	Maternal	Paternal

Eur J Med Genet. Author manuscript; available in PMC 2023 June 01.

Variants were named according to HGVS nomenclature and reference sequence NM_016023.3 (GRCh37/hg19). Abbreviations: ASM:anti-seizure medication, CBZ:carbamezapine, CZP:clonazepam, LEV:levetiracetam, PB:phenobarbital, TPM:topiramate, VPA:valproate, VNS:vagal nerve stimulation, ASD:atrial septal defect, ASDs:autism spectrum diseases, CCH:corpus callosum hypoplasia, ERG:electroretinography, GERD:gastroesophageal reflux disease, GH:growth hormone, GTC:generalised tonic clonic, HGG:hypogammaglobulinemia, IUGR:intrauterine growth retardation, NICU:neonatal intensive care unit, (I)VSD:(intra)ventricular septal defect, RVH:right ventricular hypertrophy, LGS:Lennox Gastaut syndrome, NA:not available, PEG:percutaneous endoscopic gastrostomy, PS:pulmonart stenosis, RTA:renal tubular acidosis, SGA:small gestational age, TEF:tracheoesophageal fistüle, TOF:tetrology of fallot, VSD:ventricular septal defect

*: seizure types are not available for each case; however seizures denoted in the literature are frequently characterized with generalized tonic clonic. DEL:chr8: 92,084,087-92,202,186 (GRCh37).